

The optimal helium fraction for air–helium gas mixture HDDs

Kyoung-Su Park¹

Received: 17 September 2015 / Accepted: 29 September 2015 / Published online: 7 October 2015
© Springer-Verlag Berlin Heidelberg 2015

Abstract Helium-filled drives have recently been commercialized to enable a high recording density. However, because the use of helium increases production costs, binary gas mixtures such as air–helium have been investigated. In this paper, the dominant performance metrics of hard disk drives (HDDs) are the windage losses, the flow induced vibration (FIV), the lubricant transfer and lubricant depletion. These were investigated for air–helium gas mixtures as a function of the helium fraction. The frictional torque was empirically derived in both the laminar and turbulent regimes. The windage loss and the FIV of a helium-filled drive were found to be similar to that using an air–helium gas mixture with a helium fraction of 0.75. On the other hand, the quantity of accumulated lubricant and the maximum lubricant depletion in a helium fraction of 0.75 were superior to those in a helium fraction of 1.0. Further investigation of performance metrics should be carried out. However the performance metrics considered here showed that a helium fraction of 0.75 was favorable to a helium fraction of 1.0.

1 Introduction

Magnetic information storage companies are continually working to improve the recording density of storage media in response to growing demand for big data, and the ubiquitous nature of clouding computing. Because of their

high storage density, low cost and high reliability, hard disk drives (HDDs) remain the most effective solution to meet current storage demands. To increase recording density, HDDs commonly use two tracks, which increases the bits per inch (BPI) and tracks per inch (TPI). It is particularly important to decrease the spacing between the head and media to improve the BPI. The dominant obstacles to decreasing the spacing are the lubricant accumulation on the bottom surface of slider and lube depletion. However, off-track flow-induced vibration (FIV) and windage losses induced by frictional forces should be reduced to further increase the TPI in HDDs. All of these should be simultaneously considered to increase overall storage density and improve power consumption in HDDs.

Helium-filled drives have recently been commercialized to enable a high recording density (Coughlin 2015). Such HDDs are filled with helium rather than air. Helium is the second lightest gas (after hydrogen), with a molecular weight seven times smaller than that of air. This can improve the FIV by a factor of seven because of the small momentum of the gas. In addition, helium has a larger thermal conductivity than air (Jiaping et al. 2010), and during operation the internal temperature of a helium-filled HDD is around 4 °C lower than an air-filled drive. For these reasons, helium provides small windage losses, low shear forces and favorable heat dissipation characteristics. Therefore, helium-filled drives exhibit better off-track vibration, thermal characteristics and power consumption, all of which leads to an increased TPI and better cooling performance. The use of helium in HDDs allows us to overcome the existing limit of four disk stacks; furthermore, commercialized helium-filled HDDs have included up to seven platters in a single 3.5-inch HDD, giving a total capacity of up to 8 TB.

✉ Kyoung-Su Park
pks6348@gachon.ac.kr

¹ Department of Mechanical Engineering, Gachon University,
1342 Seongnamdaero, Sujeong-gu, Seongsam-si,
Gyeonggi-do 461-701, Korea

However, the use of helium increases production costs, and may have a negative influence on head-disk interface (HDI) due to the accumulation of lubricant, lubricant depletion and poor thermal flying controller (TFC) efficiency (Nan et al. 2011). These effects are important, as they may have a negative impact on the BPI.

To achieve a balance between performance and cost, binary gas mixtures such as air–helium have been investigated (Park et al. 2013a). The dominant performance metrics of HDDs are the windage losses (which correspond to the power consumption), the FIV (which limits the off-track vibration and the TPI), and the lubricant transfer and lubricant depletion (which limit the mechanical flying height and BPI). Here, these are investigated for air–helium gas mixtures as a function of the helium fraction. Gas mixture equations are derived, and the properties of air–helium mixtures are calculated. These are then used to determine the windage losses and internal gas flow characteristics, taking consideration of the Reynolds number of the gas flow. Furthermore, the FIV is calculated as a function of the helium fraction. Furthermore, equations are derived to describe lubricant accumulation, and lubricant accumulation and depletion are calculated as a function of helium fraction. An optimal air–helium gas mixture is determined for 3.5-inch HDDs with a rotation speed of 7200 rpm.

2 Properties of air–helium gas mixtures

Here we use the variable soft sphere (VSS) model to describe a mixture of air and helium molecules, where the diffusion-based effective diameter can be calculated using Eq. (1). To consider the effects of temperature, the VSS model includes a more realistic description of contact between molecules than the hard sphere model. The mean free path of the air–helium mixture is given by:

$$d_{ref} = \left[\frac{3(\alpha_{ha} + 1)(2kT_{ref})^{\omega_{12}}}{16\Gamma(7/2 - \omega_{ha})(\pi m_r)^{1/2}n(D_{ha})_{ref}(2E_t)^{\omega_{ha}-1/2}} \right]^{1/2}, \quad (1)$$

where m_r is the reduced mass, α_{ha} is the exponent of the cosine of the deflection angle in the gas mixture, and $\omega_{ha} = 0.82$ and $\alpha_{ha} = 1.72$.

The diffusion coefficient of the binary gas mixture at low pressures is given by (Bird 1994; Park et al. 2013a, b):

$$D_{ha} = 0.00266T^{3/2} \left[\frac{1}{M_a} + \frac{1}{M_h} \right]^{1/2} / p\sigma_{ha}^2\Omega_D, \quad (2)$$

where P is pressure, σ_{ha} is the characteristic length and Ω_D is the diffusion collision integral. And M_a and M_h represent each molecular weight of air and helium, respectively. Using the VSS model with a diffusion-based effective

diameter of the binary gas mixture, the mean free path for the air–helium gas mixture is given by:

$$\lambda_m = \sum_{i=1}^2 \frac{n_i}{n} \left[\sum_{j=1}^2 \pi(d_{ref})^2 n_j \left(\frac{(T_{ref})_{ij}}{T} \right)^{\omega_{pq}-1/2} \left(1 + \frac{m_i}{m_j} \right)^{1/2} \right]^{-1}, \quad (3)$$

where i (or j) = 1 indicates air, i (or j) = 2 corresponds to helium, and d_{ref} is the reference diameter of the two molecules, which can be determined using Eq. (1). The VSS model used here includes the effects of temperature, as well as realistic gas contact phenomena and a diffusion-based effective diameter (Bird 1994; Park et al. 2013a; Park 2015).

Reichenberg’s equations represent a consistently accurate rigorous theoretical model of the viscosity of gas mixtures, and a multicomponent mixture viscosity was derived using Reichenberg’s equations with a power-law (Poling et al. 2001; Park et al. 2013a; Park 2015); i.e.,

$$\mu_m = \sum_{i=1}^2 K_i \left(1 + 2 \sum_{j=1}^2 H_{ij}K_j + \sum_{j=1 \neq i}^2 \sum_{k=1 \neq i}^2 H_{ij}H_{ik}K_jK_k \right), \quad (4)$$

where

$$K_i = \frac{y_i\mu_i}{y_i + \mu_i \sum_{k=1 \neq i}^2 y_k H_{ik} [3 + (2M_k/M_i)]}, \quad (5)$$

$$H_{ij} = \sqrt{\frac{(M_i M_j / 32)}{(M_i + M_j)^3}} Z_{ij} \left(\frac{M_i^{0.25}}{\sqrt{\mu_j Z_{ji}}} + \frac{M_j^{0.25}}{\sqrt{\mu_i Z_{ii}}} \right) \quad (6)$$

and

$$Z_{ij} = \frac{[1 + 0.36T_{rij}(T_{rij} - 1)]^{1/6}}{(T_{rij})^{1/2}}, \quad (7)$$

and where $T_{rj} = T/T_{cj}$, $T_{ri} = T/T_{ci}$, $T_{rij} = T/(T_{cj}T_{ci})^{0.5}$, T is the temperature of the gas, T_{cj} is the critical temperature of helium and T_{ci} is the critical temperature of air.

Figures 1 and 2 show the calculated properties of an air–helium gas mixture as functions of the helium fraction and of temperature. As shown in Fig. 1, the mean free path increased markedly as the helium fraction increased. This is because the mean free path of helium is approximately three times larger than that of air. The viscosity increased linearly with the helium fraction up to a fraction of 0.75, and then decreased, as shown in Fig. 2. As a result, the viscosity of the air–helium gas mixture was at maximum for a helium fraction of 0.75. This is important because it has consequences for the windage losses, FIV and the accumulated lubricant, as these depend on the viscosity deeply.

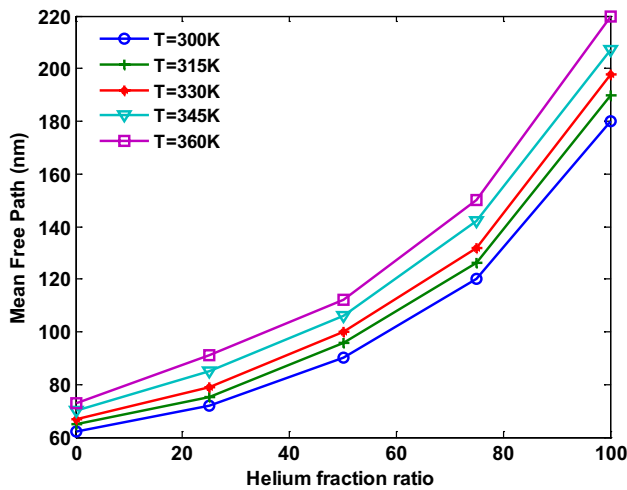


Fig. 1 Mean free path of air–helium gas mixtures (Park et al. 2013a)

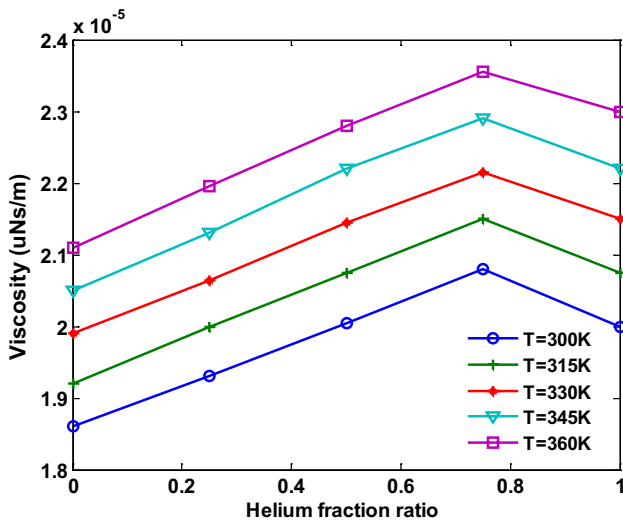


Fig. 2 Viscosity of air–helium gas mixtures (Park et al. 2013a)

3 Investigation of windage losses and flow-induced vibration

3.1 Windage losses

The boundary layer along the surface of a rotating disk can be characterized by the Reynolds number, Re . The flow in the neighborhood of a rotating disk in an HDD becomes turbulent for $Re = \rho_m V D / \mu_m > 2 \times 10^4$ (Keiji et al. 2007), where V is the linear velocity, D is the diameter of the rotating disk and ρ_m is density of the air–helium gas mixture. The flow is laminar in the neighborhood of a rotating disk for $Re < 2 \times 10^4$.

With laminar flow, we may estimate the balance of viscous and centrifugal forces, and the torque is given by $M \approx \rho U^2 R^3 (UR/\nu)^{-1/2}$. The frictional torque for the laminar case can be expressed empirically as follows (Hermann 1979; Keiji et al. 2007; Zhang et al. 2015):

$$M = 0.968 \rho_m \left(\frac{\mu_m}{\rho_m} \right)^{1/2} R^4 \omega^{5/2}, \tag{8}$$

where, ω is the angular velocity, R (38.7 mm) is the radius of the disk, and the kinematic viscosity can be described by using the relation ($\nu = \mu/\rho$) with dynamic viscosity.

With turbulent flow, we describe the velocity distribution of the air–helium mixture using a 1/7th power law. A fluid particle rotating in the boundary layer is acted upon by a centrifugal force per unit volume with a magnitude $\rho R \omega^2$. The shear stress τ_0 forms an angle θ with the tangential direction, and the radial component can be derived as follows (Hermann 1979):

$$\tau_0 \sin \theta = \rho R \omega^2 \delta, \tag{9}$$

and the tangential component of the shear stress is given by:

$$\tau_0 \cos \theta \sim \rho (\omega R)^{7/4} (\nu / \delta)^{1/4}. \tag{10}$$

From Eqs. (9) and (10), the thickness of the boundary layer $\delta \sim R^{3/5} (\nu / \omega)^{1/5}$ can be obtained, and the frictional torque of the turbulent flow can be described using

$$M \sim \tau_0 R^3 \sim \rho R \omega^2 (\nu / \omega)^{1/5} R^{3/5} R^3. \tag{11}$$

Assuming that the variation of the tangential component of the velocity of the boundary layer in the rotating disk obeys the 1/7th power law, with turbulent flow the viscous torque for the disk can be found as follows (Hermann 1979; Keiji et al. 2007; Zhang et al. 2015):

$$M = 0.036 \rho_m \left(\frac{\mu_m}{\rho_m} \right)^{1/5} R^{23/5} \omega^{14/5}. \tag{12}$$

Using the frictional torque, the power consumption may be obtained as follows (Zhang et al. 2015):

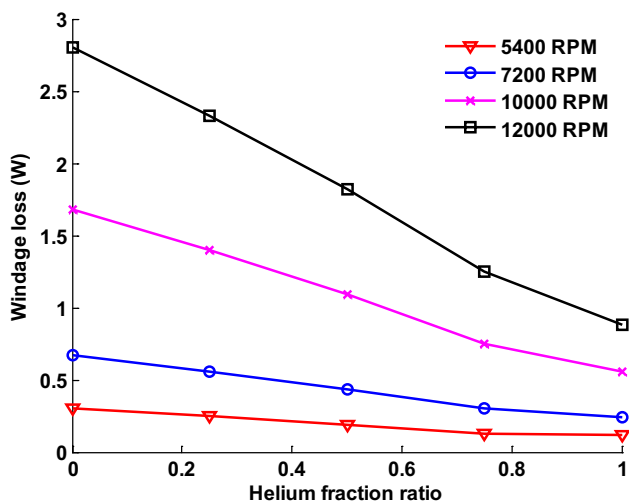
$$P_0 = M \times \omega. \tag{13}$$

This expression represents the power consumption when the disk is rotating on a co-axial cylinder with a smooth internal surface. Although this expression differs from that for the surface with a covered top and a base plate, Eq. (13) can be used to describe the power consumption for an air–helium gas mixture.

Using the above equations and the gas properties obtained above, simulations were carried out to calculate windage losses as functions of the helium fraction and the

Table 1 The simulation parameters at 300 K

Parameters	Values
Density of air ρ_a and helium ρ_h (kg/m ³)	1.164, 0.161
Dynamic viscosity of μ_a and μ_h (Ns/m ²)	186, 200
Rotational speed (rpm)	5400–12,000
Critical temperature T_c (K) of air and helium	132.53, 5.19
Hamaker constants A_1 and A_2 (J)	4×10^{-20} , 7×10^{-20}
Amplitude of polar force γ_0 (mN/m)	2.5
Molecular weight of lube M_n (kDa)	2.1
Lubricant thickness t_d (nm)	1.2
Bonding ratio of lube α_d and α_s	0.6, 0.2
Mechanical spacing FH (nm)	1.5
Linear velocity U (m/s)	31.4
Distance of closest approach d_0 (nm)	0.28
Temperature T (K)	300–360

**Fig. 3** Windage loss as functions of helium fraction and rotaion speed

rotating speed. Table 1 summarizes the parameters used in the simulation.

Figure 3 shows the windage losses as a function of the helium fraction. The windage loss decreased as the helium fraction increased, which can be explained by considering that the frictional drag forces decreased because of the low molecular weight of helium, and by considering the laminar flow characteristics of high helium fractions. For helium fractions of ≤ 0.75 , the flow was turbulent for all rotational speeds except 5400 rpm. At 5400 rpm, the flow was laminar for helium fractions of 0.75 and 1.0. For helium fractions < 0.75 , the windage losses induced by frictional drag were generally larger than those with laminar flow. With a helium fraction of 1.0, the flow was laminar for all rotational speeds. It follows that the frictional drag force is a small component of the windage losses. Therefore, an

HDD with a larger helium fraction is expected to exhibit better performance in terms of power consumption.

As shown in Fig. 3, the difference between turbulent flow (with a helium fraction of 0.75) and laminar flow (with a helium fraction of 1.0) was small ($< 5\%$) in the transitional region at low rotation speeds (5400 or 7200 rpm) because the viscosity in a helium fraction of 0.75 is bigger than that in a helium fraction of 1.0 as shown in Fig. 2.

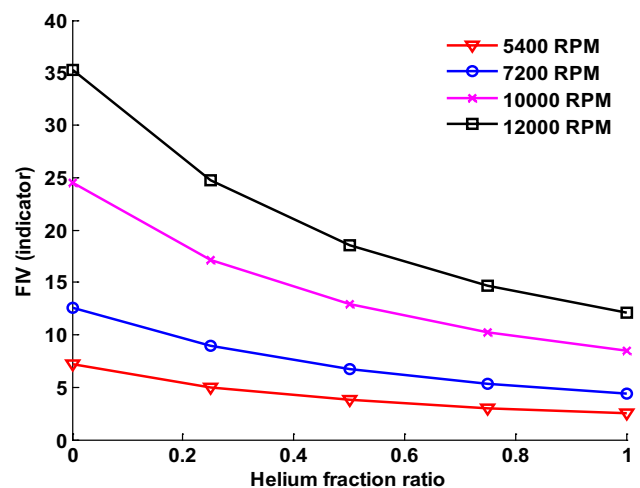
Overall, the windage losses of a helium-filled drive were similar to those of an air–helium mixture with a helium fraction of 0.75.

3.2 Flow induced vibration

Flow induced vibration is the dominant factor affecting track misregistration (TMR). We investigated the FIV for an air–helium gas mixture by calculating the FIV indicator using aerodynamic frictional force theory (Yamaguchi et al. 1986). The drag force in the rotating disk can be described using:

$$F_p = \frac{1}{2} \rho_m V^2 C_d A, \quad (14)$$

where C_d is the drag coefficient, ρ_m is the density of the air–helium gas mixture, V is the linear velocity relative to the gas in the tangential direction of the disk rotation, and A is the cross-sectional area of the head stack assembly (HSA), which depends on the system characteristics such as the number and shape of HSAs. The effect of A can be ignored for the same system. The FIV indicator is required to determine the FIV for an air–helium mixture, and because the density is inversely proportional to the product of the mean free path and A (Kyo and Kazuaki 2009), the FIV indicator can be calculated from the relationship

**Fig. 4** FIV indicator as functions of helium fraction and rotaion speed

between the velocity and mean free path of the gas using the following expression:

$$FIV \propto \frac{V^2}{\lambda} \tag{15}$$

The characteristics of the FIV for an air–helium mixture can be described using this indicator. The FIV indicator reflects the TMR characteristics, including repeatable runout (RRO) and non-repeatable (NRRO) (Kyo and Kazuaki 2009) for various disk rotation speeds, as shown in Fig. 4.

The FIV indicator decreased markedly as the helium fraction increased; however, as the rotation speed increased, the decrement of this relationship became smaller. In particular, the FIV indicator for a helium fraction of 0.75 was similar to that for a helium fraction of 1.0. This is because the Reynolds number transition occurred for helium fractions between 0.75 and 1.0 for rotational speeds of 5400 or 7200 rpm. At this transition, the FIV induced by laminar flow was slightly larger than that with turbulent flow. At 7200 rpm, the flow was turbulent with a helium fraction of 0.75, but laminar for a helium fraction of 1.0. This result is similar to the behavior of the windage losses. As a result, there was very little difference between helium fractions of 0.75 and 1.0 in terms of the FIV.

4 Investigation of the amount of accumulated lubricant and lubricant depletion

4.1 Accumulated lubricant

The shear stress on the air-bearing surface (ABS) was calculated as a function of the helium fraction using a modified Reynolds equation (Park 2015). The shear stress was used to calculate the lubricant thickness, which is related to the lubricant transfer. We considered a 3.5-inch ABS model of a Pemto slider, which operates at 7200 rpm. The operating conditions were a rotation speed of 7200 rpm, an outer diameter of 38.7 mm and a skew angle of 12.5°. The mechanical spacing of the head was 8.5 nm without TFC, and was 1.5 nm with TFC. The pitch angle was 160 μrad with air.

Figure 5a–c shows the distribution of the shear stress at the bottom surface of the slider at 300 K for helium fractions of 0, 0.75 and 1.0. In cases of pure air and a helium fraction of 0.75, the maximum shear stress at the trailing pad were around 4.2 and 3 kPa, respectively. And it was only 2 kPa in case of a helium fraction of 1.0. The maximum shear force reduced as the helium fraction increased. This is consistent with the previous simulation results for the frictional drag force.

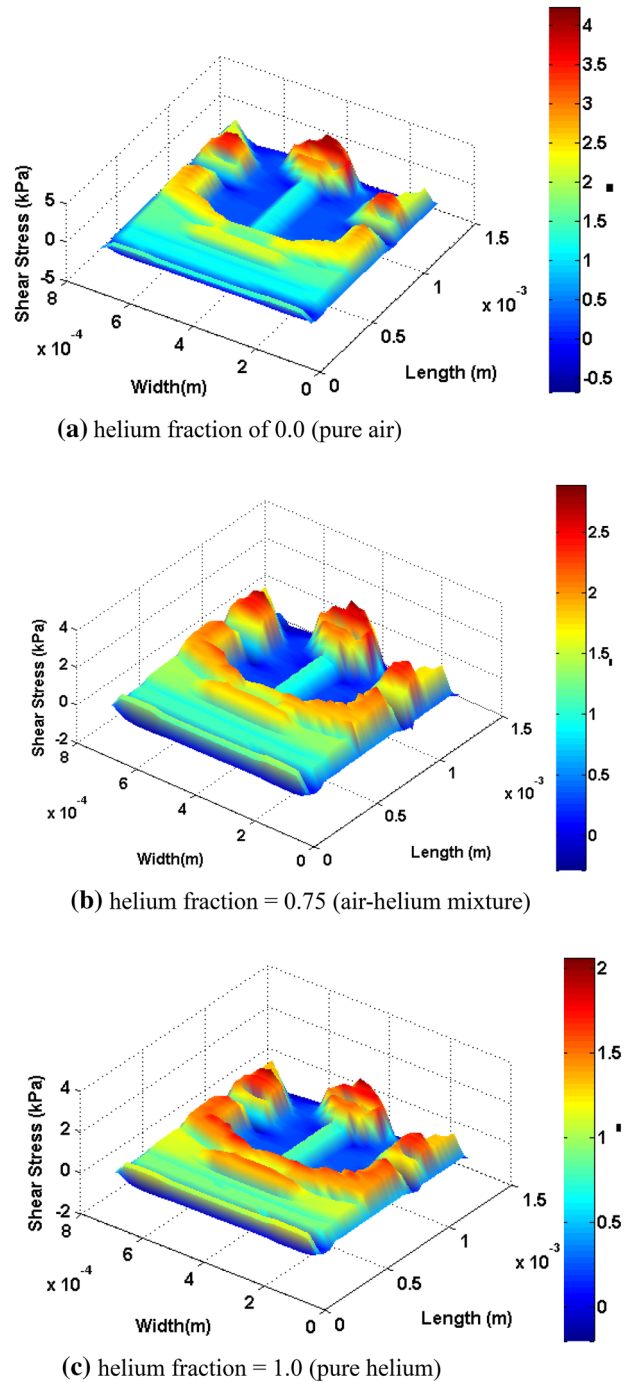


Fig. 5 Shear force distribution on the ABS surface for some cases of helium fraction

Although the windage losses and power consumption can be reduced by using pure helium (due to the small shear drag force), this may lead to lubricant accumulation (Park 2015), which can cause HDI. We simulated the lubricant accumulation as a function of helium fraction for a 3.5-inch slider operating at 7200 rpm. The mechanism for

lubricant accumulation on the slider surface is described in (Bruno et al. 2003; Ma and Liu 2007, 2008; Park 2015), and Park et al. gave a mathematical description. The main cause of lubricant accumulation is the disjoining force; i.e., the Van der Waals force between the surface and lubricant. Here we consider both dispersive and polar attractive forces. The disjoining pressure is given by (Rohit et al. 2008; Park 2015):

$$\Pi = \frac{A_1}{6\pi t_d^3} + \frac{A_2}{6\pi(FH - t_d)^3} + \frac{\pi\gamma_0}{h_0} \times \sin\left(\frac{\pi h}{h_0}\right), \quad (16)$$

where A_1 is the Hamaker constant for the lubricant/disk interaction, A_2 is the Hamaker constant for the lubricant/slider interaction, t_d is the thickness of the layer of lubricant, FH is the mechanical spacing between the head and slider, γ_0 is the amplitude of the oscillatory component of the polar energy, and h_0 is the dewetting thickness. We considered the lubricant Zdol, which has a molecular weight of 2.2 kDa. The expressions describing lubricant transfer and accumulation are as follows (Bruno et al. 2003; Ma and Liu 2007, 2008; Park 2015); for evaporation from the disk, we have:

$$N_{vapor_disk} = \frac{P_{vapor}}{kT} (1 - \alpha_d) \frac{D_d}{D_l} \cdot \exp\left(\frac{-\Pi_{disk} M_n}{\rho RT}\right), \quad (17)$$

for evaporation from the slider, we have:

$$N_{vapor_slider} = \frac{P_{vapor}}{kT} (1 - \alpha_s) \frac{D_s}{D_l} \cdot \exp\left(\frac{-\Pi_{slider} M_n}{\rho RT}\right), \quad (18)$$

and the volume flux of condensation of the lubricant is given by:

$$R_{cond_disk} = \left(1 - \frac{S_{s1}}{S_s}\right) \frac{N_{vapor_disk}}{\rho N_0} \sqrt{\frac{RT M_n}{2\pi}}. \quad (19)$$

Condensed lubricant is removed due to the shear force, and Poiseuille flow occurs due to the pressure gradient and Couette flow, which is related to disjoining pressure gradients. Assuming a tangential slip-velocity boundary condition, the shear stress can be described as follows (Ma and Liu 2007, 2008; Park 2015):

$$\tau_x = -\frac{1}{2} \frac{\partial P_{gas}}{\partial x} h + \frac{\eta_{gas} U}{h + 2\lambda_{gas}}, \quad (20)$$

where, η_{gas} is the viscosity, λ_{gas} is the mean free path of the gas molecules and U is the velocity of the surface of the disk.

The flow flux of lubricant in the x -direction on the slider surface due to the stress τ_x can be calculated using:

$$V_x = \frac{\tau_x t_s^2}{2\eta_{lube}^{eff}}, \quad (21)$$

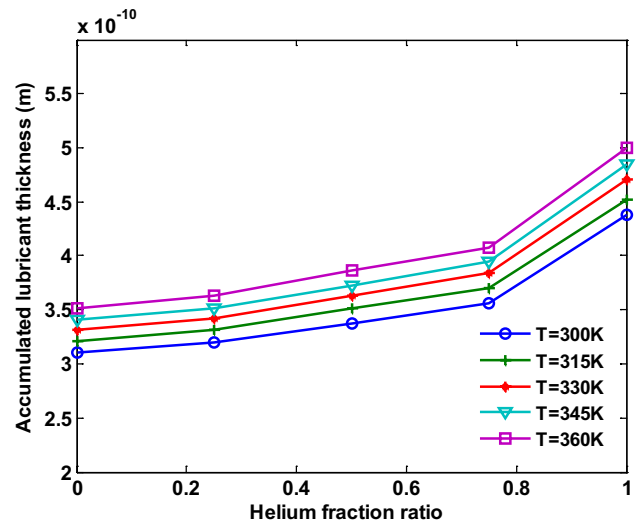


Fig. 6 Accumulated lubricant thickness as functions of helium fraction and temperature

where η_{lube}^{eff} is the effective surface viscosity of the lubricant and t_s is the accumulated thickness of the lubricant at equilibrium. The stress τ_y and the flow flux of lubricant V_y in the y -direction can be calculated in the same way. Using these expressions, the quantity of accumulated lubricant can be calculated as a function of the helium fraction and of temperature. The parameters used in this simulation were determined from (Bruno et al. 2003; Ma and Liu 2007, 2008; Park 2015).

Figure 6 shows the simulated quantity of accumulated lubricant. For helium fractions in the range 0.0–0.75, the increase in thickness was small because of high shear force; the mean free path increased exponentially as a function of the helium fraction and the viscosity also increased. On the other hand, the mean free path increased and the viscosity decreased for helium fractions in the range 0.75–1.0 as shown in Figs. 1 and 2. As a result, the shear stress decreased markedly in the range, and therefore a helium fraction of 0.75 may be considered superior to a helium fraction of 1.0 because the flying height will decrease, leading to an increased BPI.

4.2 Lubricant depletion

On diamond-like carbon there exists a thin lubricant layer to reduce friction and wear at the HDI. As long as the slider head does not make contact with the surface of the disk during read, write or floating, the bearing pressure supporting the gram load beneath the trailing pad and disjoining pressure are the dominant forces determining depletion of the lubricant film (Remmelt et al. 2001; Rohit and David 2006) because of the high pressure gradient (approximately

20 atm). Therefore, it is essential to have a clear understanding of lubricant depletion between the mobile lubricant and the flying head due to the large bearing pressure. The bearing force depends on the helium fraction because it also depends on the properties of the gas, such as the mean free path and viscosity, as described in the previous section. The bearing pressure was calculated using the modified Reynolds equation (see Sect. 4). The evolution of the thickness of the lubricant film can be determined by considering lubricant flow due to the ABS pressure and the shear force.

Mass balance for the lubricant flow in the x -direction (i.e., along the length of the slider) and the y -direction (i.e., along the width of the slider) is described as follows (Lin 2006; Choi et al. 2015):

$$\frac{\partial h}{\partial t} + \frac{\partial q_x}{\partial x} + \frac{\partial q_y}{\partial y} = 0. \tag{22}$$

The volume flow rate of lubricant per unit length in x -direction is given by:

$$q_x = \int_0^{h_l} u dz = -\frac{1}{3\mu_l} \frac{\partial(p_b + p_d)}{\partial x} h_l^3 + \frac{\tau_x}{2\mu_l} h_l^2, \tag{23}$$

and that in the y -directions is given by:

$$q_y = \int_0^{h_l} v dz = -\frac{1}{3\mu_l} \frac{\partial(p_b + p_d)}{\partial y} h_l^3 + \frac{\tau_y}{2\mu_l} h_l^2, \tag{24}$$

where u and v are lubricant velocities and τ_x and τ_y are the shear stresses in the x - and y -directions, respectively, h_l is the thickness of the lubricant, μ_l is the viscosity of the lubricant, p_b is the bearing pressure and p_d is the disjoining pressure (Lin 2006; Choi et al. 2015).

Recent experimental results (Lin 2006) have shown that the lubricant depletion profile is almost uniform in the x -direction. It follows that, after the lubricant volume has been redistributed by the pressure and shear forces during the initial stage of lubricant depletion, the lubricant thickness remains constant because the lubricant volume is conserved. Therefore, from Eq. (22), $\partial h/\partial t = 0$ and $\partial q_x/\partial x = 0$ in the steady state and $\partial q_y/\partial y = 0$. If the skew angle is small, the shear force in the y -direction can be neglected, and assuming that the shear force for the y -direction is zero (i.e., $\tau_y = 0$), Eq. (22) can be solved to calculate the evolution of the lubricant thickness due to the bearing force and the disjoining pressure. The result is that $P_b + P_d$ is constant; i.e.,

$$\frac{\partial q_y}{\partial y} = \frac{\partial(p_b + p_d)}{\partial y} = 0. \tag{25}$$

The bearing pressure can be calculated as a function of helium fraction using the modified Reynolds equation, and the disjoining pressure can be calculated as a function of the helium fraction using Eq. (16). Finally, the lubricant

Table 2 Flying attitude, maximum bearing pressure and lube depletion as a function of helium fraction

Helium fraction	0	0.25	0.5	0.75	1.0
Flying height (nm)	8.50	7.33	7.64	6.33	4.56
Pitch angle (μ rad)	161	161	158	153	144
Max. bearing pressure (atm)	20.9	22.5	22.3	24.0	26.6
Max. Δ lube depletion (nm)	0.397	0.410	0.408	0.423	0.441

thickness is calculated as a function of helium fraction ratio for lubricant thickness of 1.2 nm in steady-state.

Table 2 lists the flying attitude and bearing pressure as a function of helium fraction with static conditions. The flying height and pitch angle reduced as the helium fraction increased, to meet the balance between the supporting (bearing) force and gram load. This is because the low molecular weight of helium gives rise to a small supporting (bearing) pressure, which leads to a reduction in the spacing between the slider and lubricant. As a result, the flying height decreases and the supporting pressure increases as the helium fraction increases. The large bearing pressure caused by a large helium fraction results in increased lubricant depletion, as shown in Fig. 7. Furthermore, as shown in Table 2, the change in the maximum lubricant depletion at the trailing pad was small as the helium fraction changed from 0.0 to 0.75; however, it increased by approximately 4.3 % as the helium fraction increased from 0.75 to 1.0. In the region between 0.75 and 1.0, this might result in HDI problems such as flying instability and contact.

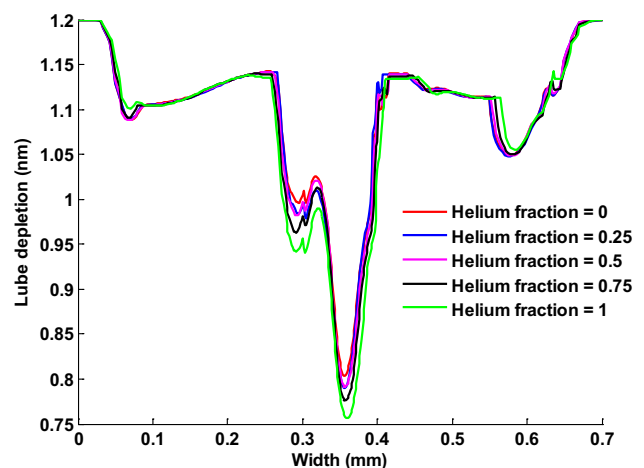


Fig. 7 Lube depletion along the width-direction of slider for helium fraction

5 Conclusions

We calculated the mean free path for an air–helium gas mixture using the VSS model with a diffusion-based effective diameter, where the viscosity was based on a binary mixture derived using Reichenberg’s equation and a power law.

The frictional torque was empirically derived in both the laminar and turbulent regimes. We then carried out simulations to calculate windage losses as functions of the helium fraction and the rotating speed. The windage losses decreased as the helium fraction increased, and the performance of a helium-filled drive was found to be similar to that using an air–helium gas mixture with a helium fraction of 0.75.

To investigate the FIV characteristics for air–helium gas mixtures, the FIV indicator was derived using aerodynamic frictional force theory. The FIV indicator decreased markedly as the helium fraction increased; however, there was little difference between helium fractions of 0.75 and 1.0.

The quantity of accumulated lubricant increased slightly as a function of the helium fraction in the region 0.0–0.75, and then increased sharply in the region 0.75–1.0. We therefore conclude that a helium fraction of 0.75 is superior to 1.0 in terms of the BPI.

The evolution of the thickness of the lubricant film was calculated by considering the lubricant flow due to the ABS pressure and shear force. We found that the maximum lubricant depletion at the trailing pad changed only slightly as the helium fraction increased from 0.0 to 0.75; however, it increased significantly in the region 0.75–1.0.

Further investigation of performance metrics should be carried out; however the performance metrics considered here showed that a helium fraction of 0.75 was favorable to a helium fraction of 1.0 (i.e., pure helium).

Acknowledgments This research was supported by Basic Science Research Program through the National Research Foundation of Korea (NRF) funded by the Ministry of Science, ICT & Future Planning (2015037574).

References

Bird GA (1994) *Molecular gas dynamics and the direct simulation of gas flow*. Oxford University Press, New York

- Bruno M, Tom K, Qing D, Rummelt P (2003) A model for lubricant flow from disk to slider. *IEEE Trans Magn* 39:2447–2449
- Choi J, Park K, Park N, Park Y (2015) Flying stability of a slider with a damaged diamond like carbon layer induced by confined optical energy in a thermally assisted magnetic recording system. In: MIPE2015 conference proceeding
- Coughlin Tm (2015) New digital storage solutions enable growing consumer applications. *IEEE Consum Electron Mag* 4:107–109
- Hermann S (1979) *Boundary-layer theory*. McGraw-Hill, New York
- Jiaping Y, Cheng P, Eng H (2010) Thermal analysis of helium-filled enterprise disk drive. *Microsyst Technol* 16:1699–1704
- Keiji A, Masaya S, Keishi S, Toru W (2007) A study on positioning error caused by flow induced vibration using helium-filled hard disk drives. *IEEE Trans Magn* 43:3750–3755
- Kyo A, Kazuaki U (2009) Written-in RRO and NRRO characteristics in mobile hard disk drives. *IEEE Trans Magn* 45:5112–5117
- Lin W (2006) Modeling and simulation of the interaction between lubricant droplets on the slider surface and air flow within the head/disk interface of disk drives. *IEEE Trans Magn* 42:2480–2482
- Ma Y, Liu B (2007) Lubricant transfer from disk to slider in hard disk drives. *Appl Phys Lett* 90:143516
- Ma Y, Liu B (2008) Dominant factors in lubricant transfer and accumulation in slider-disk interface. *Tribol Lett* 29:119–127
- Nan L, Jinglin Z, David B (2011) Thermal flying-height control sliders in air–helium gas mixtures. *IEEE Trans Magn* 47:100–104
- Park K (2015) Analysis of accumulated lubricant for air–helium gas mixture in HDDs. In: MIPE2015 conference proceeding
- Park K-S, Choi J, Park NC, Park YP (2013a) Effect of temperature and helium ratio for performance of thermal flying control in air–helium gas mixture. *Microsyst Technol* 19:1679–1684
- Park K, Choi J, Park Y, Park N (2013b) Thermal deformation of thermally assisted magnetic recording head in binary gas mixture at various temperatures. *IEEE Trans Magn* 49:2671–2676
- Poling BE, Prausnitz JM, O’Connell J (2001) *The properties of gases and liquids*, 5th edn. McGraw-Hill, New York
- Rummelt P, Bruno M, Steve M, Vamsi V (2001) Formation of lubricant “moguls” at the head/disk interface. *Tribol Lett* 10:133–142
- Rohit P, David B (2006) Lubricant depletion and disk-to-head lubricant transfer at the head-disk interface in hard disk drives. In: STLE/ASME 2006 international joint tribology conference, pp 1519–1526
- Rohit P, David B, Qing D, Bruno M (2008) Critical clearance and lubricant instability at the head-disk interface of a disk drive. *Appl Phys Lett* 92:033104
- Yamaguchi Y, Takahashi K, Fujita H (1986) Flow induced vibration of magnetic head suspension in hard disk drive. *IEEE Trans Magn* 5:1022–1024
- Zhang Q, Sundaravadivelu K, Liu N, Jiang Q (2015) Method of quick prediction of windage power loss. In: MIPE2015 conference proceeding